

Modeling droughty soils at regional scales in Pacific Northwest Forests, USA

Chris Ringo^{a,*}, Karen Bennett^{b,1}, Jay Noller^a, Duo Jiang^c, David Moore^{b,2}

^a Department of Crop and Soil Science, 109 Crop Science Building, Oregon State University, Corvallis, OR 97331, United States

^b United States Department of Agriculture Forest Service, Pacific Northwest Region, Portland, OR, United States

^c Department of Statistics, Oregon State University, Corvallis, OR, United States



ARTICLE INFO

Keywords:

Soil moisture drought
Soil moisture deficit
Evapotranspiration
Logistic regression
Landscape model

ABSTRACT

Natural resource managers need better estimates of water storage and supply in forested landscapes. These estimates would aid planning for management activities that maintain and enhance forest health and productivity and help prepare forested landscapes for a changing climate. In particular, low soil moisture in combination with high evaporative demands can induce significant stresses on forests, increasing vulnerability to attacks of insect and disease, as well as increasing wildfire risk. Although high-resolution soils data exist for much of the Pacific Northwest, regional-scale datasets that identify forested areas potentially vulnerable to soil moisture-related drought do not exist. In this study, we used readily available spatial datasets depicting available water supply, soil depth, and evapotranspiration to model the likelihood that soils experience prolonged summer drying. To calibrate the model, we examined soil profile descriptions, lab data, and soil moisture curves for 25 sites throughout the Pacific Northwest and estimated the average annual number of days that soil moisture drops to levels at or below the permanent wilting point, a theoretical lower limit of plant-available water. Using this approach, we found statistically significant relationships between the independent variables and broad classes of soil moisture levels representing the highest and lowest levels of plant-available moisture. We then used these relationships to create a landscape-level droughty soil index for the Pacific Northwest. We expect that this approach can be further developed to include additional soil moisture data outside Washington and Oregon and enhanced with other explanatory variables such as topographic position, elevation, and vegetation type. With the addition of vegetation-related data, in particular, the current modeling approach can aid in identifying vulnerable landscapes in the context of managing for increased forest resiliency in the Pacific Northwest.

1. Introduction

Soil moisture modulates the complex dynamics of the climate–soil–vegetation system and controls temporal and spatial patterns of vegetation (Noy-Meir, 1973). Soil plays a key role in this system by controlling the partitioning of moisture between inputs and outflow including runoff, evapotranspiration, and flow between organisms. Different soil types store and transmit moisture inputs and outputs differently based on their individual properties that govern water holding capacity and climatic influences. The moisture storage function of soils is particularly important in the Pacific Northwest, as over two-thirds of the region's precipitation occurs between October and March, with an average of less than two inches of rainfall occurring in the summer months.

Plants depend on soil water to carry out critical biological functions, as plant physiology is directly linked to water availability. Insufficient

water supplies create a water-stressed condition in plants. Plants under stress decrease both their transpiration and photosynthesis in an effort to balance nutrient needs and water loss. The stressed condition leaves them vulnerable to insect attack and, if prolonged, hydraulic failure and death of the plant (Choat et al., 2012).

Loss of soil water by evaporation or transpiration or both is controlled or at a minimum influenced by physico-chemical properties, surface slope and aspect, and biological demand (Hillel, 2003). We generally think of soils as “droughty” when the balance of inputs, losses, and transformations of available soil water is frequently less than the biological demand during the period of interest. Note that this notion of “droughtiness” does not refer to drought conditions per se, i.e. conditions of *uncharacteristically* long or severe moisture deficits. Rather, a droughty soil is one that consistently (chronically) has low seasonal moisture levels, and may therefore be particularly vulnerable when drought does strike. Keeping this distinction in mind, we will use

* Corresponding author.

E-mail address: Chris.Ringo@OregonState.edu (C. Ringo).

¹ Retired.

² Current address: United States Department of Agriculture Forest Service, Prescott National Forest, Prescott, AZ, United States.

the terms “droughty soil” and “drought-vulnerable soil” interchangeably, and refer to such soils as having a high soil moisture drought potential. In the Pacific Northwest, we have a climate marked by dry summers, and so we are interested in summer soil moisture in particular, and its relationship to climate and soil properties.

In practice, the term “droughty soil” is often used imprecisely, referring to a fast-draining or coarse-textured soil, or one that does not receive adequate water recharge relative to vegetation and evapotranspirational demands. The USDA Natural Resources Conservation Service (NRCS) defines soil drought vulnerability in terms of agricultural crops in their metadata for the gridded Soil Survey Geographic Database (gSSURGO; *Soil Survey Staff, 2016a*): “Drought vulnerable soil landscapes comprise those map units that have available water storage within the root zone for commodity crops that is less than or equal to 6 in. (152 mm).” This definition, however, does not include any consideration of climatic influence. In the metadata’s referenced publication (*Dobos et al., 2012*), it is stated that, “... If the soil receives timely rainfall, AWC (available water-holding capacity) is less important,” explicitly indicating that a full definition of a droughty soil requires the consideration of at least the quantity of precipitation occurring during the growing period. As climatic gradients in the Pacific Northwest can be extremely sharp both seasonally and geographically, we would argue that including climatic considerations in any definition of soil droughtiness is critical. In this work we develop a definition of a droughty soil derived from class breaks in our calibration dataset, and show that this results in a better indication of soil droughtiness than using available soil water storage alone.

The forest management benefits of understanding which landscapes and which soil types have a high soil moisture drought potential are many. Increasing forest growth potential, improving forest resiliency to climate change induced drought and improving prediction of wildfire potential are some key management applications of this work. In addition, knowledge of landscapes with droughty soil helps land managers prioritize limited budget allocations. In this way, managers can ensure that vegetation treatments which reduce forest stand density and decrease fuel loads are targeted to areas where they will be most effective in improving forest health and resilience to climate change.

Chase et al. (2016) found that thinning of dense forest vegetation increased soil moisture during the summer months on their study sites in northern Idaho and northeastern Washington. They found that “thinning high-density stands on low productivity sites will provide the greatest stress relief and benefit to overall forest health because resources are more limited and competition for those resources is high. Alternatively, thinning high productivity, high density stands will maximize the growth response of residual trees”. In addition, they found that for the studied forest types, thinning had the greatest relative impact on summer soil moisture, followed by soil N availability, and light interception. Reduced tree water stress by thinning is a viable option for increasing forest resiliency to drought induced by climate change (*D’Amato et al., 2013; Elkin et al., 2015; Sohn et al., 2013*). Other studies have found that similar soil moisture effects can be realized through prescribed burning (*Hatten et al., 2012*).

Knowledge of soil moisture conditions can also improve our ability to estimate wildfire danger. *Krueger et al. (2015)* showed that weather variables alone were insufficient to predict wildfire potential and that fire danger predictions were enhanced when soil moisture data were used. Although the authors recognized that many factors influence fire occurrence and size such as weather, ignition source, fuel characteristics, and suppression efforts, they found that soil moisture information was significantly related to fire size during the growing season. By using a measure of the fraction of available water holding capacity (FAW) of the soil to understand the influence of soil moisture on fire occurrence, they found that all size Class 5 (> 405 ha.) fires occurred at FAW less than 50 percent and that 87% of the largest fires occurred when FAW was less than 20 percent. Inclusion of soil moisture information in wildfire prediction models could improve assessments of wildfire

danger, particularly as a possible surrogate for live fuel moisture. Although the current model focusses on whole-column soil moisture, the methodology could be adapted to consider only the top portion of the column, which may be more closely associated with wildfire danger.

The primary objective of this effort was to produce a landscape-level droughty soil index that could help inform forest managers which areas are potentially vulnerable to soil moisture drought. Since we have focused here *exclusively* on modeling summer soil moisture levels, it is important to note that the model does not speak directly to vegetation stress, as plants are generally adapted to their site. Rather, we envision that this index represents one variable among many that can be used in helping managers select areas for treatment that will potentially provide the “best bang for their buck.”

2. Methods

2.1. Study area

The study covers the forested areas of the USDA Forest Service Pacific Northwest Region, including Washington and Oregon and small areas of National Forest land in northern California (the Siskiyou NF). The Pacific Northwest is a highly diverse landscape both geographically and climatically. The majority of National Forest System (NFS) lands spans seven mountainous Pacific Northwest ecoregions described in *Omernik (1987)* with minor components of NFS land present in four lowland ecoregions (*Fig. 1*). Geological diversity is expressed in rocks of different age classes dating from Jurassic to early Pleistocene and from such diverse lithologies as basalt, diorite, andesitic breccia, massive arkosic sandstone, greywacke, quartz-mica schist, peridotite and unconsolidated alluvium. Weathering, tectonic activity, mass wasting, glaciation, fluvial processes and volcanic eruptions have altered exposure of the bedrock throughout most of the study area. Volcanic soils from multiple eruptions and of varying ages and particle sizes blanket the central and eastern Cascades and areas of eastern Oregon and Washington north of Crater Lake. Common soil orders on forest lands include Inceptisols, Andisols and Alfisols. Spodosols have locally developed in coastal areas and on some upper elevation slopes in the Cascades (*Heilman et al., 1979*). Mollisols can be found in forested areas that were once open savanna.

The study area has a Mediterranean climate with most moisture falling in winter. The majority of the precipitation falls from October to February, and less than 10% occurs during July through September (*Western Regional Climate Center, 2017*). Two parallel mountain ranges, the Coast Range and the Cascade Range separate the wetter and cooler western half of the study area from the drier and warmer eastern half of the study area. The Pacific Ocean, bordering the western edge of the study area is responsible for moderating the climate from the coast to the Cascade Mountains. Winter storms move from west to east and drop significant rainfall on the windward slopes of the Coast Range and Olympic Mountains, ranging from a mean annual precipitation of 1900–2290 mm (75–90 in.) at the coast up to 5080 mm (200 in.) at the crest. Precipitation on the windward slopes of the Cascades is one half to two thirds of the coastal rainfall. On the eastern, leeward slopes of the Coast Range, Olympic, Cascade, and North Cascade mountains rainfall amounts decline sharply from 5080 mms (200 in.) in the Coast Range to 1020 mm (40 in.) in the Puget Lowlands and Willamette Valleys and from 2030 to 2540 mm (80–100 in.) at the crest of the Cascade Range to a low of 203 mm (8 in.) in the lowlands of the Columbia Plateau and Northern Basin and Range Ecoregions. The Rocky Mountains ecoregion of NE Washington and the Blue Mountains of eastern Oregon experience an increase in precipitation up to 900 mm (35 in.) due to orographic lifting and marine air moving up the Columbia River Basin.

Morning fog can occupy coastal and lowland valleys in the western portion of the study area in late summer and early fall. Because of this, solar flux is not a simple measure of aspect nor is surface soil moisture

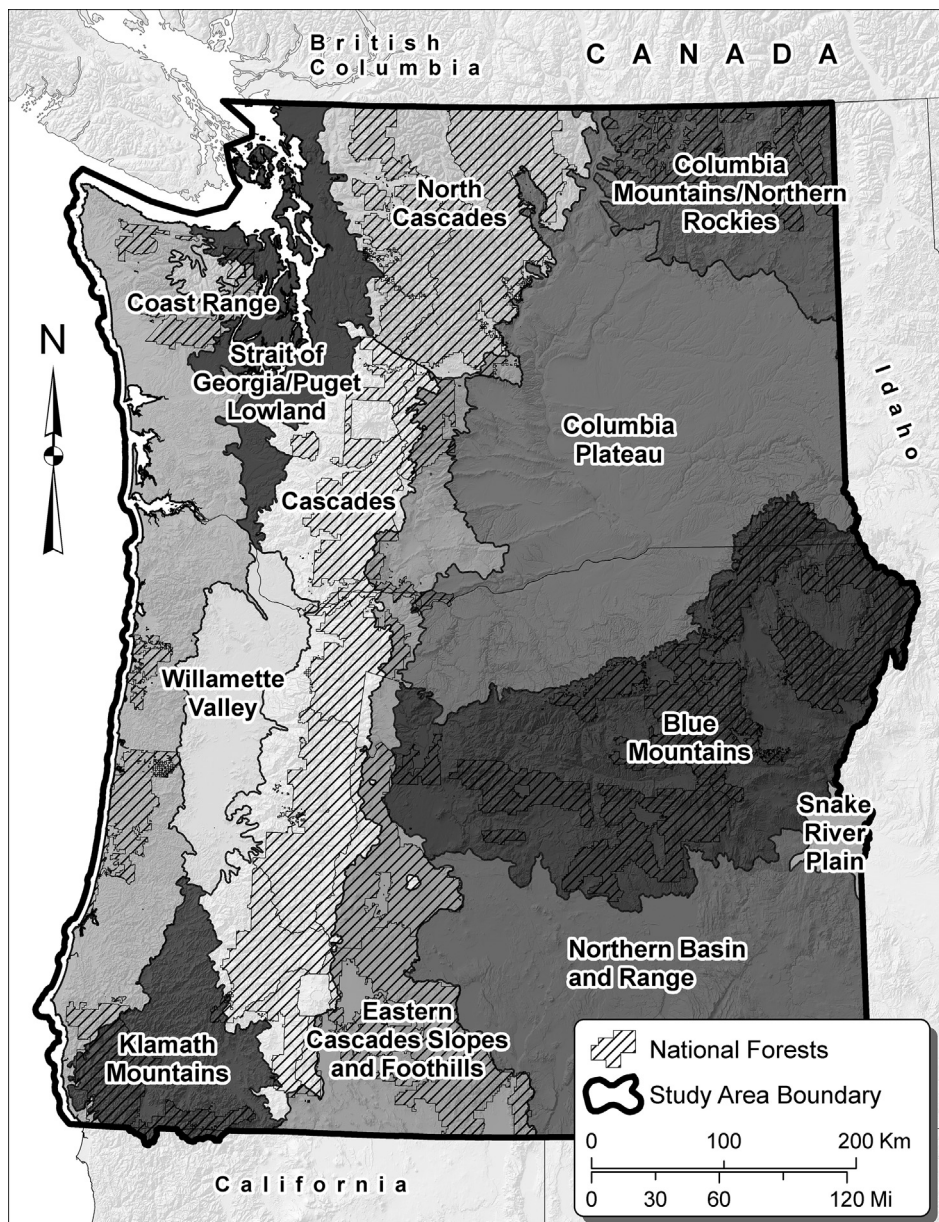


Fig. 1. Study area and Omernik ecoregions.

solely dependent on precipitation. In the coastal ecosystems of the Pacific Northwest, fog drip and foliar uptake during fog events can be a significant source of plant-available moisture during the drier summer months (Azevedo and Morgan, 1974). In addition, this coastal fog acts to increase relative humidity and suppress transpiration, and the resulting “...increase in available water and reduction of evaporative stress has a marked impact on overall ecosystem productivity” (Koraćin et al., 2014).

Snowfall increases with elevation with some of the high volcanic peaks reaching a cumulative total of 20–25 m (67–83 feet) of snowfall. Snowfall begins in the high mountains in September with maximum depths of 3–8 m (10–25 feet) accumulating in the first half of March. Pockets of snow remain on the ground at elevations above 1524 m (5000 feet) until early July.

Temperatures, too, are moderated by the Pacific Ocean in western Oregon and Washington but reach temperature extremes in the high mountains and high elevation arid deserts of eastern Oregon and Washington. The average temperature near the coast in July is 21 °C (70 °F) and 24 °C (75 °F) in the foothills, with average minimum

temperatures near 10 °C (50 °F). In the coastal regions and the western foothills of the Cascade and North Cascade Mountains, the January maximum temperatures range from 6 to 9 °C (43–48 °F) and minimum temperatures from 0 to 3 °C (32–38 °F). In contrast, mean annual summer temperatures in the inland valleys in SW Oregon and areas east of the Cascades in both Oregon and Washington range from 32 to 41 °C (90–105 °F). Mean maximum winter temperatures in those regions range from –4 to 2 °C (25–35 °F) and mean minimum winter temperatures range from –18 to –9 °C (0–15 °F). Mean minimum temperatures from –18 to –27 °C (0 to –17 °F) have been recorded at higher elevations.

2.2. Available water supply (AWS)

We began this analysis by assembling a geospatial dataset of available water supply (AWS) for the Pacific Northwest region. AWS is a measure of the total amount of plant-available moisture the soil column is capable of holding to a given depth. Knowing AWS can provide land managers with information to help them understand

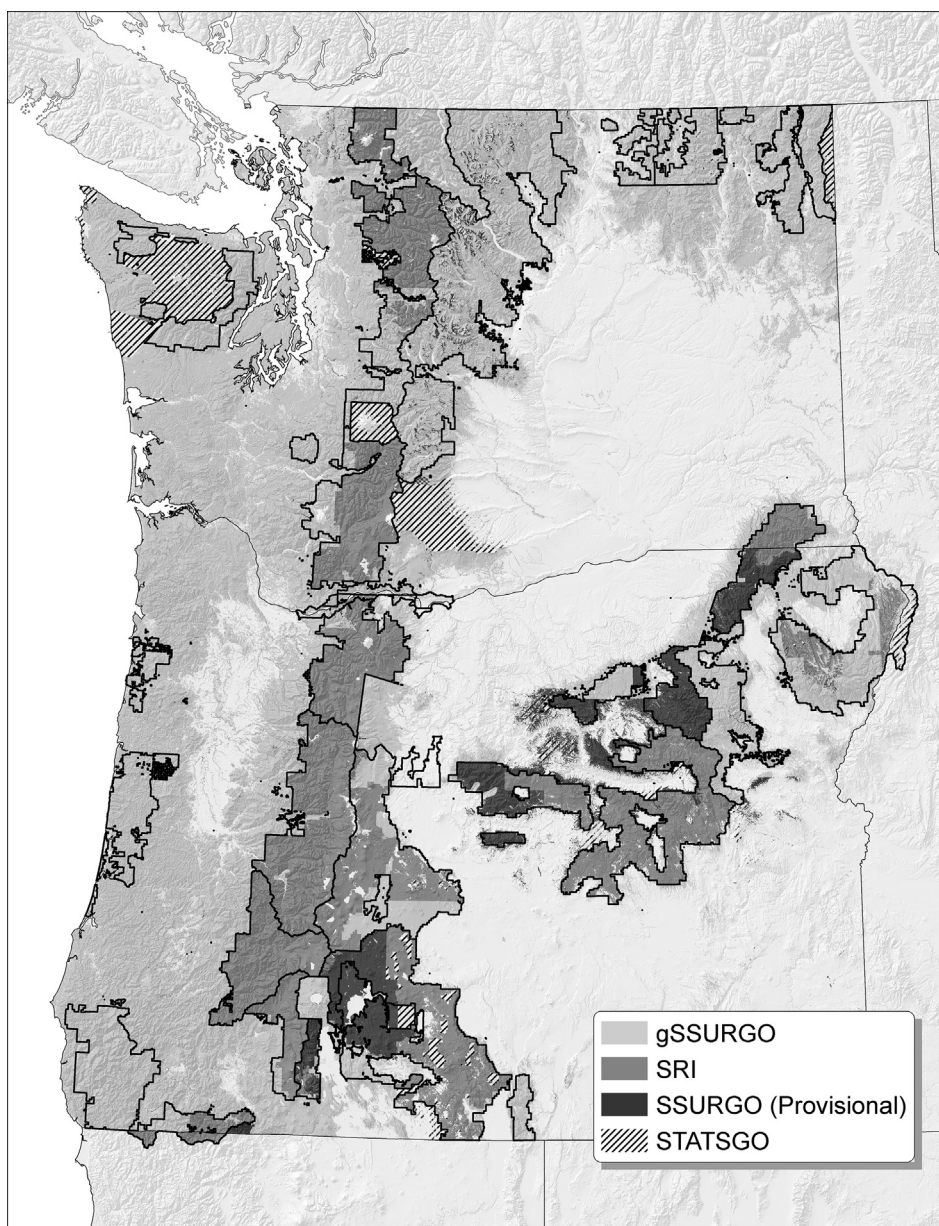


Fig. 2. Soils data sources for forested lands in the Pacific Northwest.

where on the landscape there is a high, moderate or low potential to store water in order to attenuate runoff and flooding, to understand where soil moisture may be available for plant use longer into the growing season, and to improve fire-danger forecasts. For this analysis, we adopted the standard soil survey soil profile depth of 150 cm (60 in.) or to a root-restricting layer, whichever is less.

We calculated AWS using the best available soil information in the region, which came from a combination of the National Cooperative Soil Survey data published by NRCS and USDA Forest Service Soil Resource Inventory (SRI) data (Noller et al., 2018). NRCS soils data are available for immediate use in a Geographic Information System (GIS) as either a Soil Survey Geographic (SSURGO) Database in polygon format (Soil Survey Staff, 2016b) or as a gridded Soil Survey Geographic (gSSURGO) Database in raster format (Soil Survey Staff, 2016a) at a scale of 1:24,000. Soil attributes accompany each of these data sets. Approximately two-thirds of the forested area in the region is covered by published SSURGO surveys (Fig. 2). In areas of active SSURGO surveys, the gSSURGO dataset was supplemented by provisional (unpublished) SSURGO survey data, which were obtained from the

regional NRCS office. In areas without SSURGO surveys, information from USFS SRIs at a scale of 1:63,360 was used. This merged dataset helps fill in many of the gaps in available high-resolution datasets for the Pacific Northwest (see Fig. 2).

The gSSURGO dataset includes estimates of AWS to a 150 cm (60 in.) depth, and we used these estimates where available. In the areas for which we were able to obtain provisional SSURGO data from NRCS, we used the provided representative values for Available Water Capacity (AWC) and horizon thickness for each soil horizon and calculated AWS for the major soil component, according to formula (1) below. AWC is a property of the soil horizon, and is calculated according to formula (2).

$$AWS = \sum_{i=1}^n thk_i \times AWC_i \quad (1)$$

thk_i = Thickness of horizon i
 AWC_i = AWC for horizon i

$$\text{AWC} = (W_{1/3} - W_{15}) \times (\text{Db}_{1/3}) \times \text{Cm}/100 \quad (2)$$

AWC = volume of water retained in 1 cm³ of whole soil between 1/3-bar and 15-bar tension; reported as cm/cm [numerically equivalent to inches of water per inch of soil (in/in)]

W_{1/3} = weight percentage of water retained at 1/3-bar tension

W₁₅ = weight percentage of water retained at 15-bar tension

Db_{1/3} = bulk density of < 2-mm fraction at 1/3-bar tension

Cm = rock fragment conversion factor derived from: volume moist < 2-mm fraction (cm³)/volume moist whole soil (cm³)

For areas with only SRI data, we first used Eq. (2) to compute AWC for each of the two or three soil layers recorded for each map unit, and then calculated AWS according to Eq. (1). To accomplish this, rock fragment percentages, soil layer thicknesses, and soil textures were compiled for all map units, and we then used a soil texture relationship for W_{1/3} – W₁₅ in Eq. (1) based on NRCS lab data for similar textures (see *Soil Survey Staff, 2007, pp. 115–116*). Several forests included lab data for bulk density for some or all map units, and we used these values where available. For the remaining map units, we used estimated bulk densities of 1.0 g/cc for surface layers and 1.25 g/cc for subsurface layers for mineral soils, and 0.7 g/cc for surface layers and 1.0 g/cc for subsurface layers for volcanic ash soils. The AWS values computed for the SRI-only areas are based on the major soil component only. Aside from making calculations easier, we use the dominant component because we generally have a low level of confidence in the percentages given for the components. By selecting what the soil scientist identified as the major component, we feel we are better representing AWS for the majority of the landscape.

Finally, in areas with no SSURGO or SRI data, we used STATSGO estimates (*Soil Survey Staff, 2016c*) in order to get a complete AWS dataset for the region. Fig. 3 shows the resulting AWS raster dataset (30 m resolution) for the region based on the above calculations.

2.3. Evapotranspiration

In addition to knowing AWS, it is also important to look at and understand the climatic factors that affect soil moisture availability. This includes the precipitation inputs (rain and snow) and the outputs (runoff and evapotranspiration) from the soil column. This improved soils information can ultimately be used along with precipitation and temperature data in hydrologic models, such as the Variable Infiltration Capacity (VIC) model (*Liang et al., 1994*), to better examine the interactions of climate, soil characteristics, and topography. For this analysis however, we took the simpler approach of using these finer-resolution AWS data to enhance the spatial resolution of existing broad-scale climatic indicators of potential soil moisture limitation. The climatic indicator we used is based on estimates of potential and actual evapotranspiration.

Potential evapotranspiration (PET) is an estimate of the evaporation and transpiration that would occur if an adequate supply of moisture were available. Actual evapotranspiration (AET) measures the actual loss of moisture from soil and plant surfaces, and so the degree to which AET falls below PET may be interpreted an indicator of moisture limitation (*Nagarajan, 2010, e.g.*). Therefore, we have used AET/PET in our analysis as a broad-scale climatic indicator of potential moisture deficit (Fig. 4).

We obtained modeled average monthly actual and potential evapotranspiration datasets at a 1 km resolution from the Numerical Terradynamic Simulation Group at the University of Montana. (*Mu et al., 2011*; data are available at <http://www.ntsug.unt.edu/project/modis/mod16.php>). In their MODIS Global Evapotranspiration Project, they used remotely sensed land cover, leaf area index (LAI), Fraction of Absorbed Photosynthetically Active Radiation (FPAR), and albedo data together with daily meteorological inputs of air temperature, air

pressure, humidity, and shortwave radiation to model AET and PET. Since the Pacific Northwest experiences a predominantly Mediterranean climate with very little summer precipitation, we are primarily interested here in summer moisture limitation. Over Washington and Oregon in particular, July, August, and September are the three driest months (*Western Regional Climate Center, 2017*), and so we are using these three months to represent summer in our model. We calculated the average AET/PET ratio for July-August-September for the years 2000–2014, and used these datasets as the climatic input to our droughty soil model (Fig. 4).

We chose AET/PET over average precipitation to represent climate in the model for two main reasons. First, we were looking for a variable that reflected the net result of the hydrologic cycle, rather than just moisture inputs. We felt that if we used straight precipitation it would be difficult to account for areas where snowmelt is an important moisture input later into the season, or other hydrologic processes such as surface runoff. Evapotranspiration on the other hand, reflects the outcome of these processes. Secondly, early on in our data exploration, it appeared from simple regression analyses that AET/PET would actually give a better model fit than precipitation.

Still, there are certainly downsides to using AET/PET for this application. Perhaps most obviously, it is a global-scale dataset with a one kilometer pixel size, and so its utility for regional-scale studies such as this one may certainly be questioned. But maybe more importantly, it is itself a modeled dataset with many inherent sources of uncertainty, including uncertainties stemming from biases in the model's input MODIS LAI/FPAR and daily meteorological datasets; inaccuracies in the eddy covariance flux tower data used to calibrate the model outputs; and basic limitations in the model algorithms themselves (*Mu et al., 2011*). On balance however, we felt it was a better choice for this initial study given that in theory at least, it would reflect moisture conditions on the ground in a way that precipitation alone cannot. In future versions of this model however, we will take a closer look at incorporating in-situ temperature and precipitation datasets collected at the SNOTEL site locations themselves.

2.4. Soil depth

Soil depth is an important variable in determining AWS. We assembled a spatial dataset of soil depth at a 30 m pixel size from gSSURGO data (where available), and then used SRI data to backfill, using the midpoint of the range of depths given for major soil components. Most map units in the STATSGO dataset do not have depth estimates, and so we were unable to fill in the remaining holes in the data. See Fig. 5 (note that blank areas are either non-forest areas, areas unmapped in the SSURGO and SRI datasets, or mapped SSURGO areas for which the data are not released to the public from tribal governments). As NRCS normally describes soil properties to a standard depth of 150 cm (60 in.), we recorded depths only to 150 cm or to a root-restricting layer. It should be noted that even though very few plant roots are found below this depth (*Gilman, 1990*), it is known that many tree species develop roots over great distances and are able to access deep water sources such as deep soil layers, deep water tables, and even weathered bedrock (*Maeght et al., 2013; Stone and Kalisz, 1991; Rempe and Dietrich, 2018*). However, available regional soils datasets do not describe these deeper layers and so we are not able to include these effects in our model.

2.5. Calibration dataset

To calibrate the model we used daily soil moisture data from the network of Snow Telemetry (SNOTEL) stations in Washington and Oregon. In order to arrive at a precise definition of soil droughtiness, we looked at the relationship between permanent wilting point (PWP) and soil moisture at each site. Permanent wilting point is defined as the moisture content of a soil at which plants wilt and fail to recover when

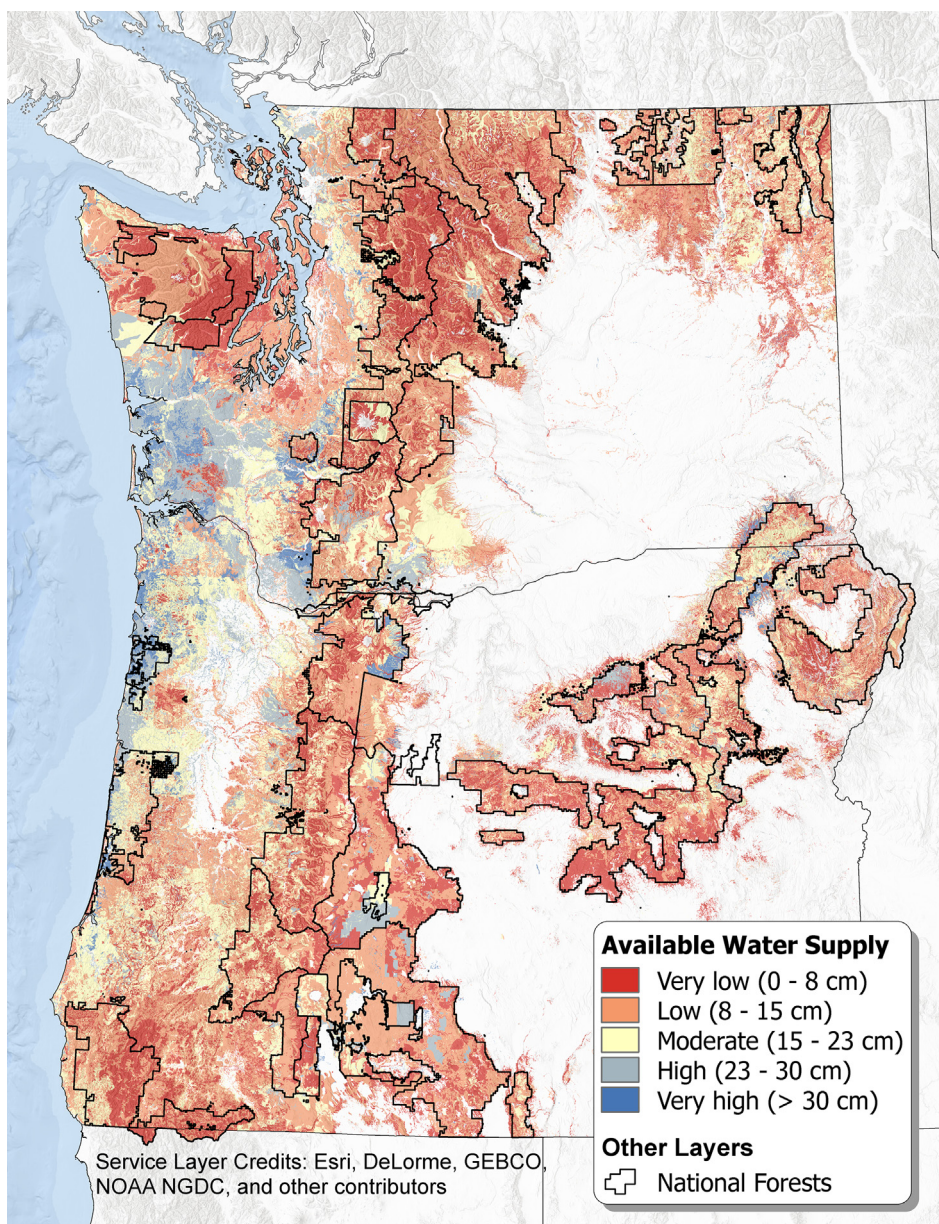


Fig. 3. Available Water Supply to a 150 cm depth or to a root restricting layer for forested lands in the Pacific Northwest.

supplied with sufficient moisture (NRCS, 2008). Using lab data published for each SNOTEL site, we computed a depth-weighted average PWP for each site, which we then compared to the soil moisture curves. We used the standard pressure of -15 bar (1.5 MPa) to compute PWP values, the theoretical pressure above which plants can no longer extract any remaining moisture from the soil. While we realize that this pressure certainly varies by plant species, our intent here is only to model soil moisture content, and not vegetative stress. See Figs. 6 and 7 for example soil moisture curves and PWP for two contrasting sites.

Of the 46 SNOTEL sites in Oregon and Washington that had soil moisture information, we used 25 sites (Fig. 8). We rejected sites for use in the calibration dataset for the following reasons: the site had less than 3 years of nearly continuous soil moisture record (small data gaps were allowed); the soil moisture sensors at the site were erratic, having long and/or frequent periods with no data; the soil moisture sensors at the site did not cover enough of the soil column to accurately calculate PWP and AWS for the entire soil column; the site is non-forested (less than 10% canopy cover); or the site had incomplete or inconsistent lab data and/or pedon description that prevented accurate calculations of

PWP and AWS.

For each SNOTEL site in the calibration dataset, we calculated the average annual number of days that the soil moisture dropped below PWP. We then calculated AWC for each soil horizon from the lab data and calculated AWS to a maximum depth of 150 cm. Then for each site we determined the modeled value of the average July-August-September AET/PET, averaged over the years matching the soil moisture record for the site. Table 1 gives the values of AWS, AET/PET, soil depth, and the years of record and annual number of days for which soil moisture was below PWP for each SNOTEL site in our calibration dataset.

3. Results

Without taking soil depth into account, initial plots of AET/PET versus AWS values for our calibration dataset indicated that as a group at least, the sites with the lowest AET/PET and AWS values correspond fairly closely with those that have the greatest number of days below PWP, at least as a group (Fig. 9).

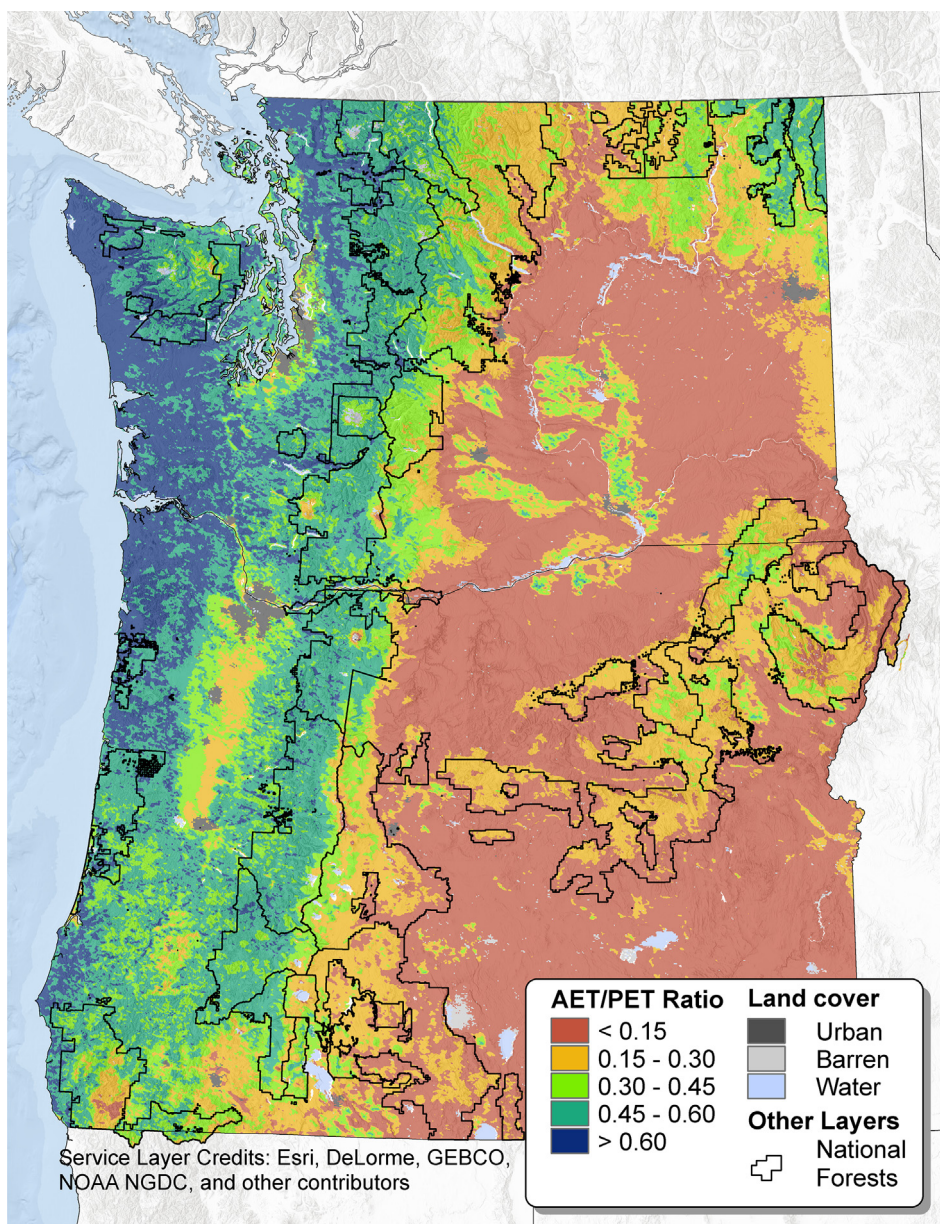


Fig. 4. Actual evapotranspiration divided by potential evapotranspiration on forested lands in the Pacific Northwest, July–August–September average, 2000–2014.

Initially we attempted to quantitatively predict the average annual number of days a site is below PWP using a weighted multiple linear regression, with the weights accounting for the number of years of the soil moisture record for each site (more years of record means more a robust estimate of annual average days below PWP). Using this approach however, the optimal model based on the Akaike Information Criterion (AIC) (Cavanaugh and Neath, 2011, e.g.) has limited predicting power, with only 42.1% of the variability across sites captured by the explanatory variables (AWC, AET/PET, and soil depth).

We then classified the sites into three categories based on the average annual number of days below permanent wilting point for that soil and defined them as: “not droughty” (not more than 3 weeks < PWP); “marginally droughty” (more than 3 weeks, but less than 10 weeks < PWP); and “droughty” (more than 10 weeks < PWP). The class breaks were chosen to give us three classes of approximately equal size, which also happened to break the dataset at reasonable gaps in the dataset. Among the 25 sites included in the analysis, nine sites are not droughty, eight are marginally droughty, and eight sites are droughty by these definitions. Fig. 8 shows the location and “droughty

status” of the calibration dataset.

In addition to AWS, AET/PET, and soil depth, we tested several related variables for inclusion in the categorical model as well. These included mean canopy cover at the site and within different radii (45 m, 90 m, and 700 m), the fraction of soil depth reached by the sensors, and whether the field capacity (FC) lab data was clod-based or based on a sieved sample. Canopy cover estimates were tested as an attempt to account for variability in evapotranspiration within a 1 km pixel, ranging in distance from a 30 m pixel at the SNOTEL site itself, up to a radius encompassing the entire 1 km pixel. Canopy cover estimates were obtained from the Gradient Nearest Neighbor (GNN) dataset (Ohmann and Gregory, 2002). The fraction of soil depth reached by the sensors was included as a possible measure of uncertainty of the column estimates of soil moisture content. Lab data for FC were derived using measurements of either sieved or clod soil samples, and since clod-based estimation of FC is preferred (Soil Survey Staff, 2014; Young and Dixon, 1966), this was included as a possible measure of uncertainty of the FC and AWS estimates. However, none of these variables turned out to contribute significantly to the model.

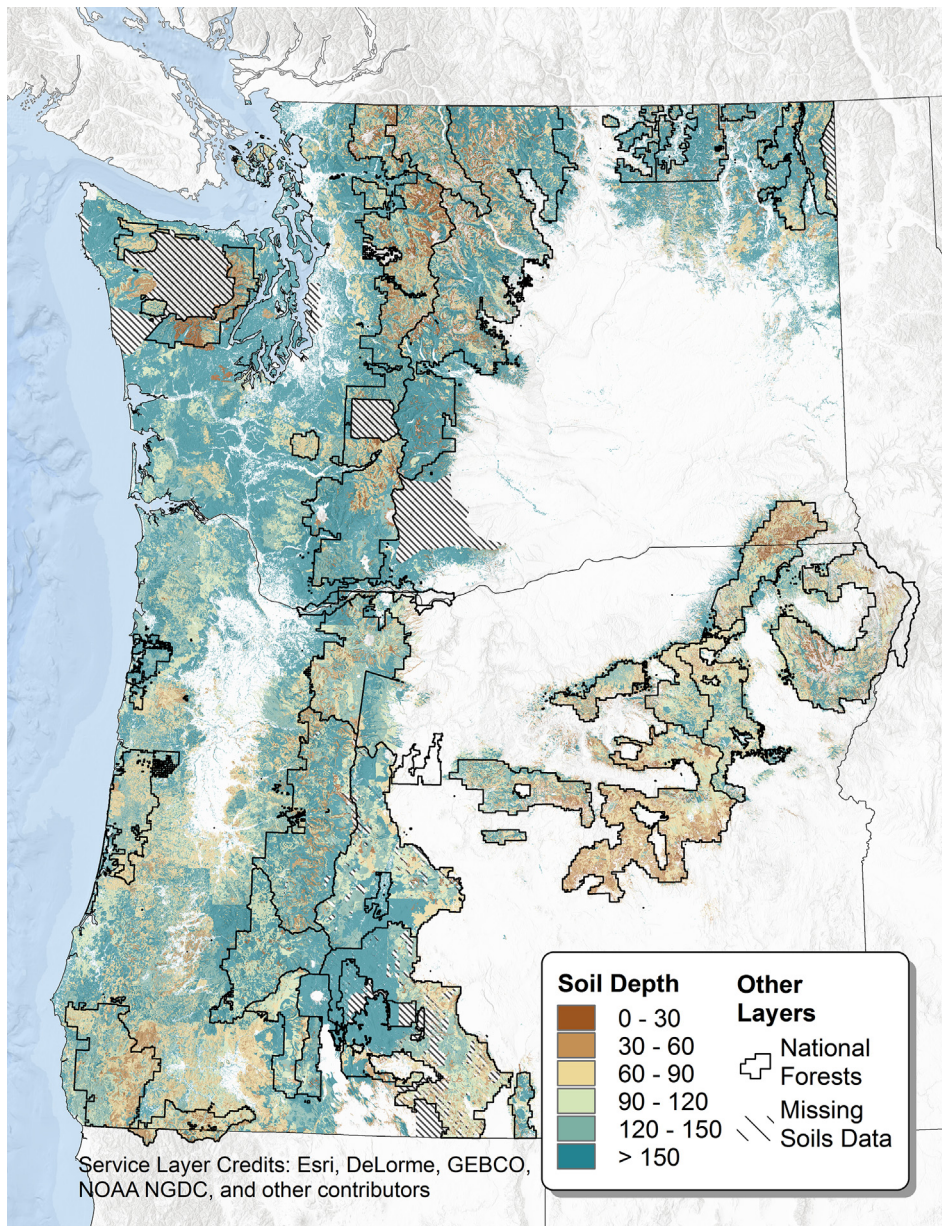


Fig. 5. Soil depth to 150 cm (60 in.), forested lands in the Pacific Northwest.

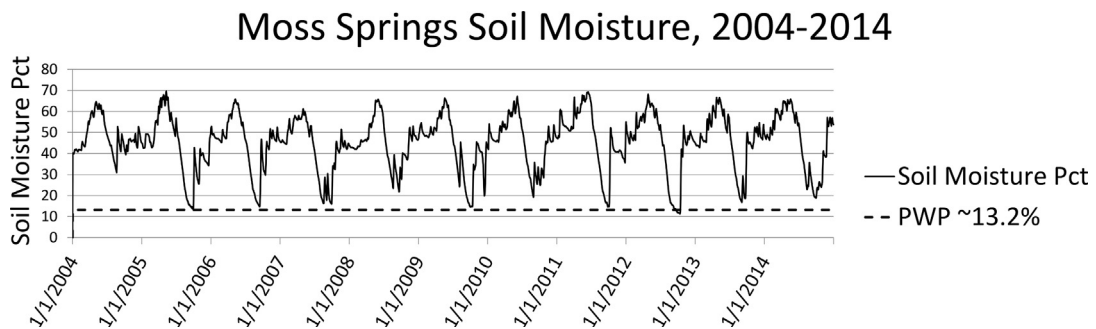


Fig. 6. Example of SNOTEL site with soil moisture remaining above PWP for most of the year (PWP ~ 13.2% for the Moss Springs site).

We used ordered ordinal logistic regression to model the ordered categorical response for droughtiness using the R statistical package (R Core Team, 2016). In the optimal model based on the AIC, droughtiness is negatively associated with AWS (two-sided p-value = 0.00028), AET/PET (two-sided p-value = 0.00046), and soil depth (two-sided p-

value = 0.010). To evaluate the fit of the model, for each site in the analysis, we take the category with the highest fitted probability as the fitted classification. It is worth noting that although AWS and soil depth are somewhat correlated (correlation coefficient of 0.48), including them both improved the model by reducing the residual deviance. And

Chemult Alternate Soil Moisture, 2004-2014

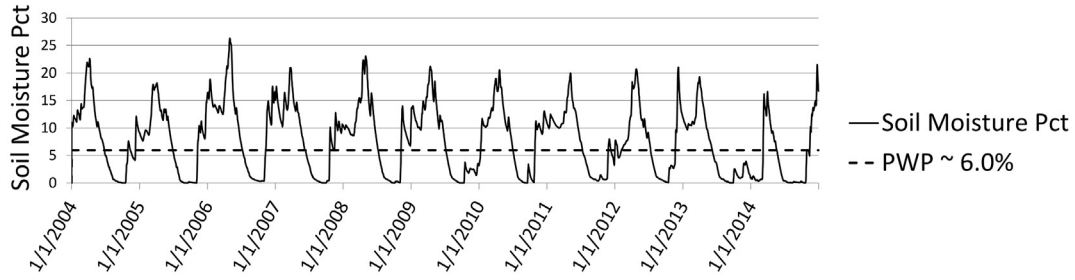


Fig. 7. Example of SNOTEL site with soil moisture dropping below PWP for significant periods of time annually (PWP ~ 6.0% for the Chemult Alternate site).

although the model fit was improved significantly less with the addition of soil depth than with either AWS or AET/PET (as evidenced by soil depth's higher p-value), we elected to keep soil depth in the model since it did improve the fit somewhat.

most of the sites with non-ambiguous droughty status, with eight out of the nine not droughty sites correctly fitted, and seven out of the eight droughty sites correctly fitted. As would be expected due to the way the sites are classified, the model is not as accurate for the sites with a less definite droughty status (six of the eight marginally droughty sites are

As shown in Table 2, the ordered logistic model is able to capture

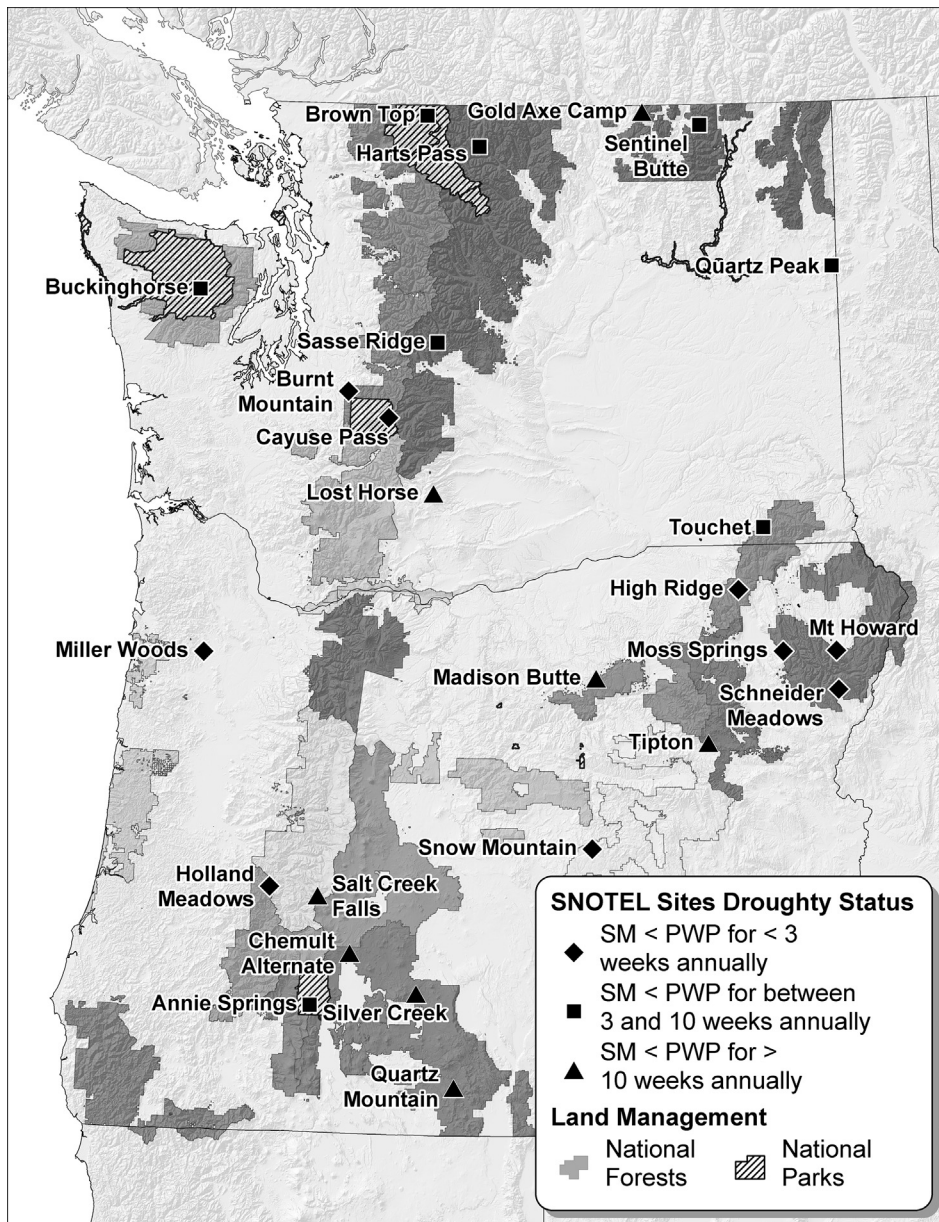


Fig. 8. Final calibration dataset: SNOTEL site droughty status.

Table 1
Site data for the 25 SNOTEL sites in the final calibration dataset, ordered by increasing number of days for which soil moisture is less than PWP.

SNOTEL site name	Years of soil moisture record	Jul-Aug-Sep AET/PET	AWS (cm)	Soil depth (cm)	Annual # of days < PWP
Cayuse Pass	2012–2014	0.44	18.77	84	0
High Ridge	2004–2014	0.38	28.78	150	0
Miller Woods	2008–2014	0.57	14.34	150	0
Mt Howard	2004–2014	0.17	14.63	150	0
Schneider Meadows	2011–2014	0.33	24.36	150	0
Snow Mountain	2005–2007	0.14	21.84	150	0
Moss Springs	2004–2014	0.28	22.93	127	2
Burnt Mountain	2009–2014	0.51	12.03	104	10
Holland Meadows	2011–2014	0.51	22.33	150	21
Brown Top	2010–2014	0.45	7.56	90	30
Sentinel Butte	2007–2014	0.36	5.62	150	37
Sasse Ridge	2005–2014	0.41	11.96	150	45
Buckinghorse	2009–2014	0.54	10.22	71	60
Harts Pass	2011–2014	0.33	20.42	106	64
Quartz Peak	2010–2014	0.47	8.64	81	66
Annie Springs	2004–2014	0.21	8.89	150	67
Touchet	2011–2014	0.30	15.59	79	73
Gold Axe Camp	2012–2014	0.18	10.54	64	88
Silver Creek	2012–2014	0.13	4.75	60	97
Lost Horse	2005–2012	0.18	4.99	48	101
Salt Creek Falls	2012–2014	0.50	4.60	53	101
Madison Butte	2009–2014	0.25	4.82	108	124
Chemult Alternate	2004–2014	0.21	14.70	150	158
Tipton	2004–2012	0.24	11.93	69	166
Quartz Mountain	2004–2014	0.17	8.59	150	174

Table 2
True and fitted classification using the ordered logistic model.

Actual droughty status	Fitted droughty status	Fitted droughty status			Total
		Not droughty	Marginally droughty	Droughty	
Not droughty	Not droughty	8	1	0	9
Marginally droughty	Not droughty	2	6	0	8
Droughty	Marginally droughty	0	1	7	8
Total	Droughty	10	8	7	25

classified as marginally droughty, while two sites are classified as not droughty). It is worth noting that none of the droughty sites was mis-fitted to be not droughty, and none of the not droughty sites was mis-fitted to be droughty. These results suggest that our model is able to distinguish between droughty and non-droughty sites with high confidence.

Fig. 10 shows the corresponding graphs of the modeled probabilities for each individual site within the three droughty classes. In each of the three graphs, the y-axis gives the modeled probability of being in each of the three classes as indicated by the color of the bars.

Fig. 10A shows the modeled probabilities for the nine “not droughty” sites, and as can be seen, it is the Mt Howard site that models incorrectly as “marginally droughty”. The Mt. Howard site is a relatively high-elevation (7900’) site located in a small forested depression on an otherwise sparsely vegetated mountain top in northeastern Oregon. During the period of record, this site never drops below 30% soil moisture (with a PWP around 10%), likely due to late snowpack, cooler temperatures, and local topographic position. Addition of both topographic position and elevation variables could help this site to model correctly.

In addition, note that although the Snow Mountain site models correctly, it is fairly close to modeling in the “marginally droughty” class. This site is at the edge of a narrow densely forested swale in an area of otherwise open canopy forest on the Malheur National Forest in

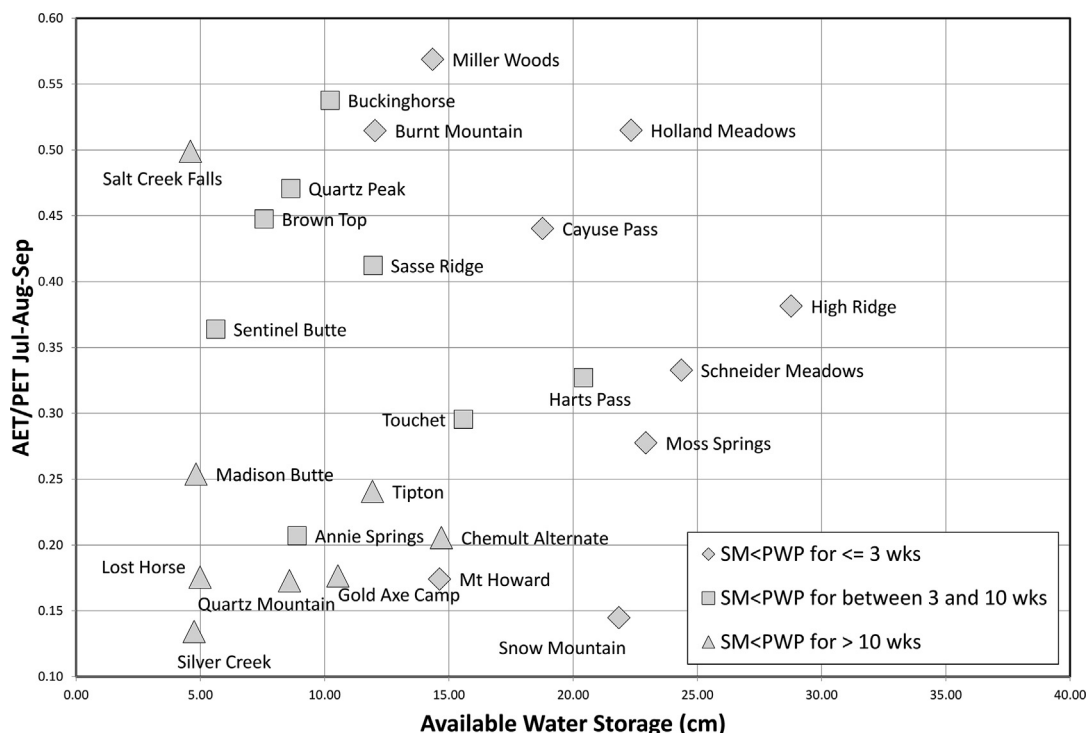


Fig. 9. AET/PET plotted against AWS for each SNOTEL site. Plots are grouped into three sets according to the number of weeks that soil moisture drops below PWP.

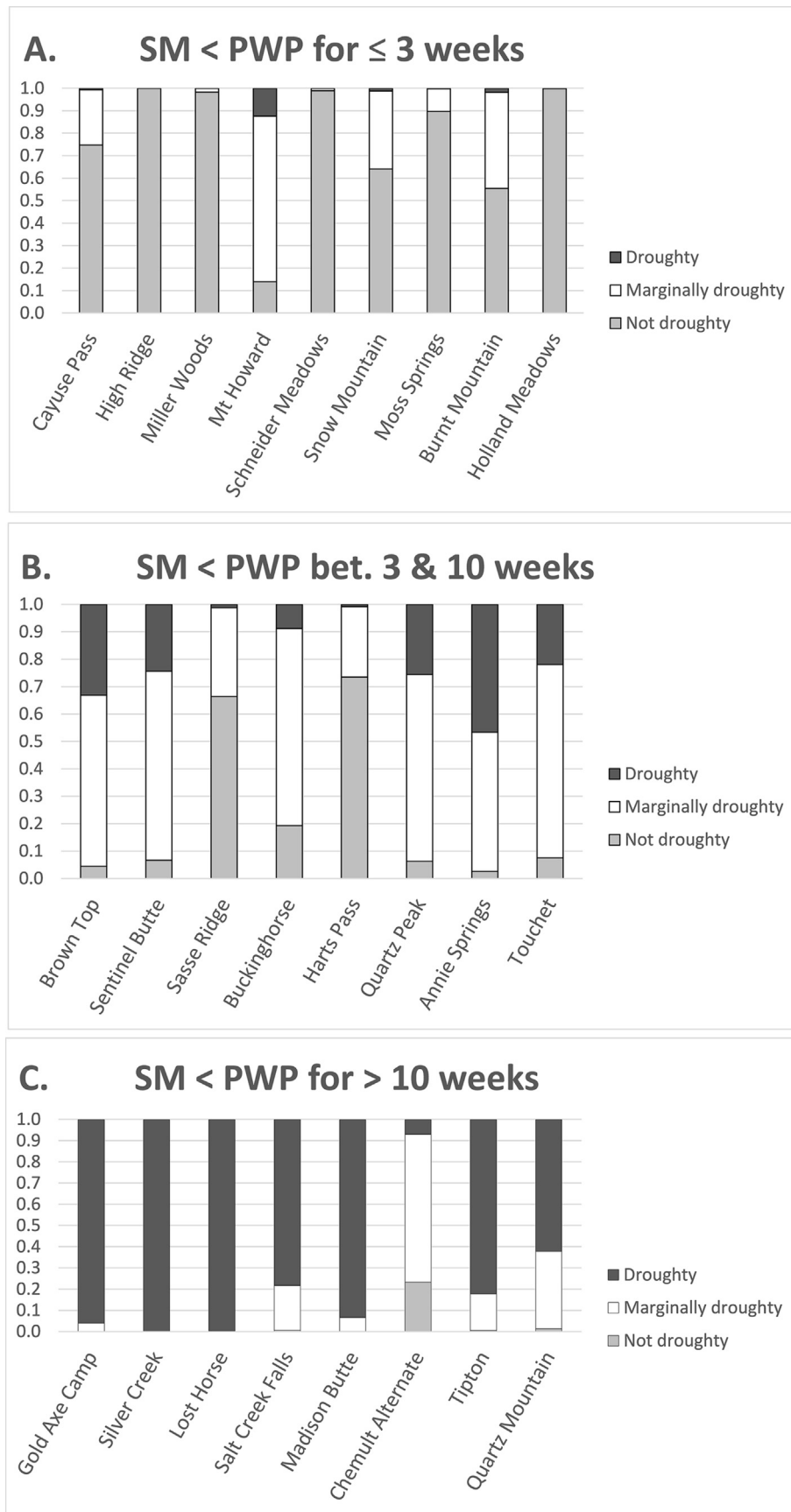


Fig. 10. Modeled soil moisture drought potential for each site. In each graph the y-axis is the fitted probability of being in each of the three classes as indicated by the color of the bars. Graph A shows the “not droughty” sites; graphs B & C show the “marginally droughty” and “droughty” sites, respectively.

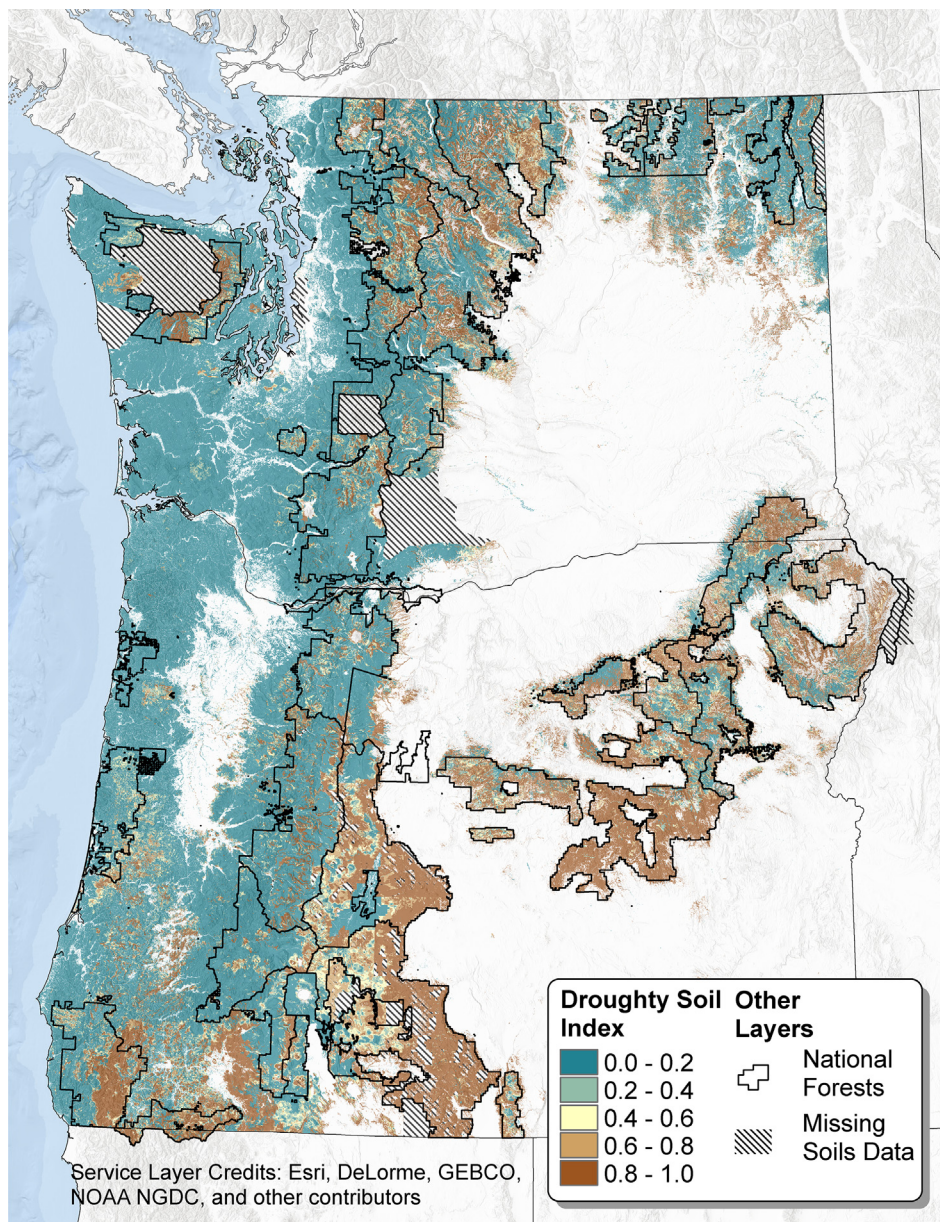


Fig. 11. Droughty soil index for forested landscapes in the Pacific Northwest.

eastern Oregon. For both this site and the Mt. Howard site, the broad-scale evapotranspiration data are not able to capture vegetation changes smaller than the 1-km resolution. Addition of a finer-scale canopy cover variable may then help to refine the model in these situations.

The Chemult Alternate site, shown in Fig. 10C, may indicate a different problem. This site is the one droughty site that does not model correctly. The site is located just northeast of Crater Lake and has deep ash soils with 25–30% pumice fragments from past eruptions of Mt. Mazama. Many authors have investigated the challenges of calibrating soil moisture sensors in coarse volcanic soils (e.g., Comegna et al., 2013; Regalado et al., 2003; Weitz et al., 1997). In particular, Stenger et al. (2005) demonstrated that standard calibrations of soil moisture sensors typically underestimate soil moisture held within pumice fragments, and so the actual available soil moisture at this site may possibly be significantly higher than that indicated by the site's soil moisture sensors (Fig. 7). Hence the number of days below PWP may well be considerably fewer in number than indicated by the sensors for this site. It is worth noting that Hydra Probe® moisture sensors by

Stevens Water Monitoring Systems (<http://www.stevenswater.com/products/sensors/soil/hydraprobe/>) are installed at all Washington and Oregon SNOTEL sites, using one of the four factory calibrations (Deborah Harms, NRCS, personal communication, March 9, 2018). According to the Hydra Probe® manual however, “Andisols, gelisols and histosols are soil that may have soil moistures and properties that depart from the Hydra Probe's built in calibration curves. If the bulk density is extremely low giving the soil an effective porosity greater than 0.5, the user will need a custom calibration”. Geist and Cochran (1991) give a generalized porosity value of .77 for central Oregon pumice soils, which suggests that a custom calibration at this site may well be warranted.

In the final landscape model, the fitted probabilities p_1 (not droughty), p_2 (marginally droughty), and p_3 (droughty) satisfy the three equations:

$$(1) p_1 + p_2 + p_3 = 1$$

$$(2) \log(p_1/(p_2 + p_3)) = \alpha_1 + \beta_1 * x_1 + \beta_2 * x_2 + \beta_3 * x_3$$

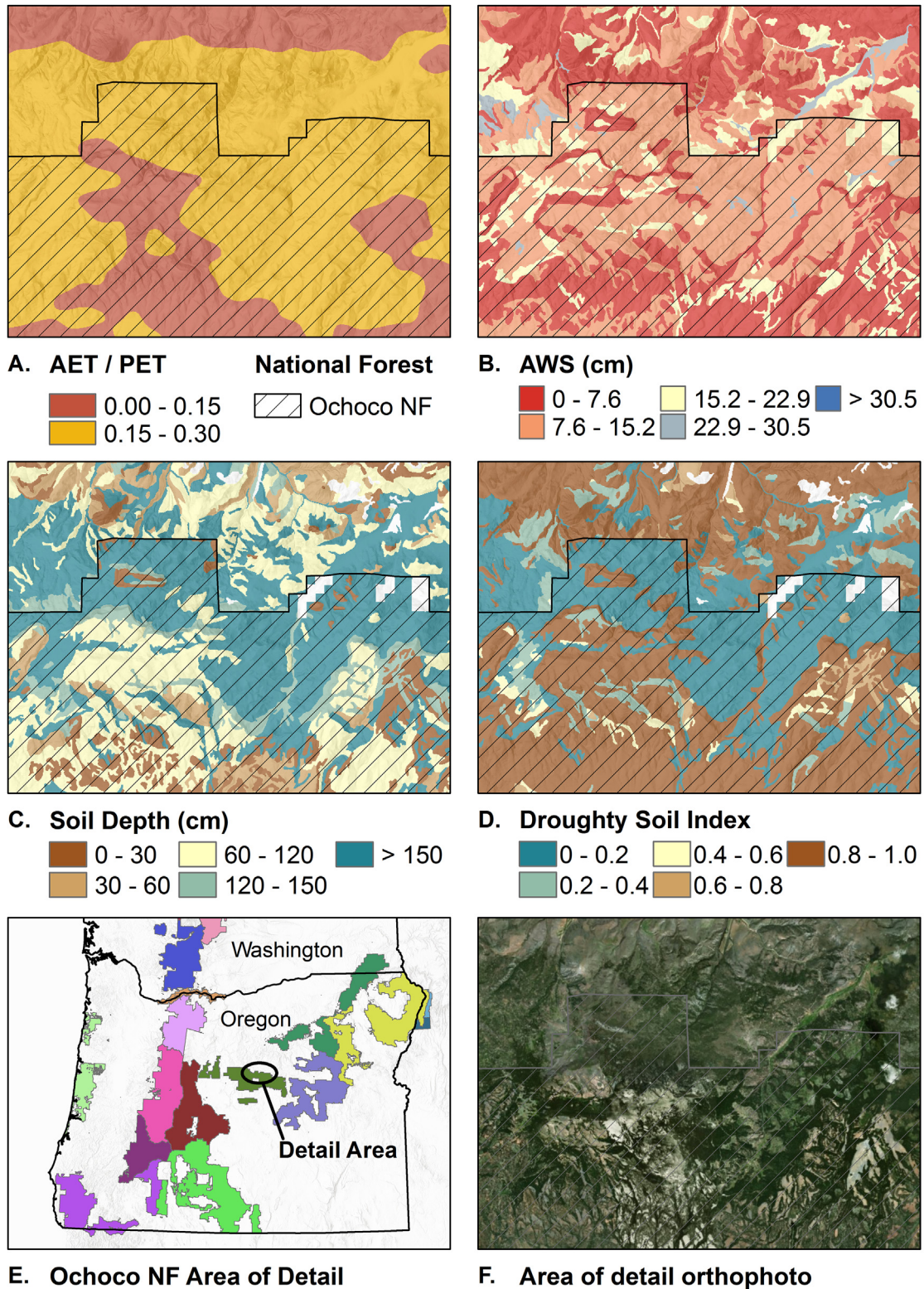


Fig. 12. North slope of Ochoco Mountains detail area.

$$(3) \log((p_1 + p_2)/p_3) = \alpha_2 + \beta_1 * x_1 + \beta_2 * x_2 + \beta_3 * x_3,$$

where x_1 is AWS, x_2 is AET/PET, x_3 is soil depth, $\alpha_1 = -16.60$, $\alpha_2 = -12.82$, $\beta_1 = 0.4065$, $\beta_2 = 14.95$, $\beta_3 = 0.04138$.

Given values for AWS, AET/PET, and soil depth, these three equations can be explicitly solved for p_1 , p_2 , and p_3 , giving us the basis for

our landscape model of droughty soils. We are primarily interested here in calculating p_3 across the landscape, the probability that a given pixel is “droughty” (i.e., that soil moisture < PWP for at an average of least 10 weeks annually). Fig. 11 shows the result of that landscape calculation.

4. Discussion

Soil information adds value to assessments of drought potential. Throughout the Pacific Northwest Region, soil-forming properties have resulted in a wide variety of soil types ranging from areas scoured to bedrock by glacial action with little to no soil formation, to areas of deep fine-grained lakebed deposits, to areas with thick deposits of pumice and ash. As a result, there are widely different abilities of different soil types to absorb, store, and supply moisture to vegetation throughout the year. Climatic stressors play a significant role in determining how much water plants need to perform critical physiologic functions. In this paper we have demonstrated that the combination of climatic information (evapotranspiration) and information on physical soil characteristics (AWS and soil depth) does a better job of identifying soils that experience prolonged periods of low summer moisture levels than either set of information does by itself. Combining soil resource characteristics with climatic information through this model improves the understanding of which portions of the landscape have a high probability to restrict moisture to plants (Fig. 11). The following example illustrates these relationships.

Referring to the maps of the north slope of the Ochoco Mountains in Fig. 12, broad-scale climatic information would lead one to conclude that actual evapotranspiration (AET) of vegetation is occurring at a low to very low rate, at less than 15% of potential evapotranspiration rates (PET) (the red areas in Fig. 11A). In the orange areas on the map, only slightly higher rates of AET are occurring at 15–30% of PET. However, when one brings in soil resource information as described above, a different picture emerges. More detailed soil information (Fig. 11B and C) in combination with the climatic information helps one understand that there are portions of this area where the soil type, in this case deep deposition of volcanic ash, results in a low probability (less than 20%) of droughty soils. These areas are indicated in dark blue on the map in Fig. 11D. These forests have higher growth potential and presumably a higher resilience to drought. In this area, volcanic ash deposition and subsequent weathering increases the ability of the soil to store and transmit moisture to plants throughout dry periods of the year.

The greater the ability of forest managers to understand which landscapes have a tendency to be droughty, the greater is their ability to improve forest management strategies. As fire frequency and size is increasing in the western United States (Dennison et al., 2014), the ability to predict fire danger is critical. Adding a soil moisture variable to that prediction improves forecasting abilities (Krueger et al., 2015). This model can help fire managers identify sites to install soil moisture sensors to assist in fire danger modeling (though as noted above, basing the analysis on just the top portion of the soil column may produce better results for this purpose). The model performed well identifying sites with the highest and lowest soil moisture drought probability. It is the areas in the middle, with less definitive soil moisture drought probabilities where a more thorough vetting of soil and climatic parameters, through establishment of a soil moisture assessment network, would gain the most information for fire managers.

Foresters too can use this modeling approach to prioritize thinning of forest vegetation to reduce soil moisture stress of high density stands. The resulting thinning operations will not only reduce fuel loads but will improve forest resilience to climate change induced drought. For areas where sustainable timber production is deemed the highest ecosystem service value, this model can assist forest managers in identifying highest priority thinning sites to increase forest growth (Chase et al., 2016). With limited budgets focused on fuels treatment and forest health improvement, tools such as this droughty soil index can provide valuable information for forest managers to use in prioritizing land management treatments to areas where they can be most effective in maintaining forest health and resilience to climate change.

5. Conclusions

This study refined our understanding of the diversity and patterns of droughty soils across forested areas of the Pacific Northwest states of Oregon and Washington. By combining NRCS and newly-acquired “legacy” USFS soil survey information, using site specific soil information from SNOTEL sites, and by using AET/PET models across the region, we were able to both develop a definition of a droughty soil and extrapolate those findings to produce a preliminary map of drought-vulnerable soils for most of the region.

There is much to be understood about soil moisture drought, and we suggest a few avenues here that could prove fruitful in helping to quantify the role of soils in drought processes affecting forested environments in the Pacific Northwest.

In terms of this specific modeling effort, there are almost 500 SNOTEL and SCAN (Soil Climate Analysis Network) sites with soil moisture data across the Western US that could be used to build a more robust model of drought-vulnerable soils. This dataset would include enough sites to partition the data into calibration and validation datasets and could be used to validate this model, and to expand it to include both forested and non-forested environments across the western US.

Another consideration is that the Pacific Northwest is unique in the western US with its volcanic landscapes. Soil moisture release curves are unique for pumice and volcanic ash-influenced soils and estimating soil moisture parameters in these soil types is difficult and not completely understood. Soil moisture and vegetative response studies in pumice and volcanic ash-influenced soils could greatly improve our knowledge of drought-vulnerable soils throughout much of the Pacific Northwest region.

Lastly, it is important to again emphasize that an indication that a soil is droughty does not necessarily imply vegetation stress, as plants are generally adapted to their site. However, as demonstrated by Choat et al. (2012), a tree's adaptation to its moisture regime is very often quite narrow, leaving forest trees across a broad range of environments potentially vulnerable to drought stress due to shifts in rainfall patterns associated with climate change. Thus a reliable droughty soil index will also be useful in helping detect thresholds beyond which certain species will falter. Future research comparing modeled future precipitation to this droughty soils index could help identify Pacific Northwest forests most vulnerable to climate change.

Acknowledgements

This work was supported by the United States Department of Agriculture Forest Service, Pacific Northwest Region [Agreement No. NFS 12-CR-11062754-017]. We thank Mark Kimsey, Jeff Hatten, Nancy Grulke, Cara Farr, and two anonymous reviewers for their thoughtful reviews of earlier versions of this manuscript.

References

- Azevedo, J., Morgan, D.L., 1974. Fog precipitation in Coastal California forests. *Ecology* 55 (5), 1135–1141.
- Cavanaugh, J.E., Neath, A.A., 2011. Akaike's information criterion: background, derivation, properties, and refinements. In: Lovric, M. (Ed.), *International Encyclopedia of Statistical Science*. Springer, Berlin, Heidelberg, pp. 26–29.
- Chase, C.W., Kimsey, M.J., Shaw, T.M., Coleman, M.D., 2016. The response of light, water, and nutrient availability to pre-commercial thinning in dry inland Douglas-fir forests. *For. Ecol. Manage.* 363, 98–109.
- Choat, B., Jansen, S., Brodribb, T.J., Cochard, H., Delzon, S., Bhaskar, R., Bucci, S.J., Feild, T.S., Gleason, S.M., Hacke, U.G., et al., 2012. Global convergence in the vulnerability of forests to drought. *Nature* 491 (7426), 752–755.
- Comegna, A., Coppola, A., Dragonetti, G., Severino, G., Sommella, A., Basile, A., 2013. Dielectric properties of a tilled sandy volcanic-vesuvian soil with moderate andic features. *Soil Tillage Res.* 133, 93–100.
- D'Amato, A.W., Bradford, J.B., Fraver, S., Palik, B.J., 2013. Effects of thinning on drought vulnerability and climate response in north temperate forest ecosystems. *Ecol. Appl.* 23 (8), 1735–1742.
- Dennison, P.E., Brewer, S.C., Arnold, J.D., Moritz, M.A., 2014. Large wildfire trends in the

- western United States, 1984–2011. *Geophys. Res. Lett.* 41 (8), 2928–2933.
- Dobos, R.R., Sinclair, H.R. Jr, Robotham, M.P., 2012. National Commodity Crop Productivity Index (NCCPI) User Guide, Version 2. Available from: <http://www.nrcs.usda.gov/Internet/FSE_DOCUMENTS/nrcs142p2_050734.pdf> .
- Elkin, C., Giuggiola, A., Rigling, A., Bugmann, H., 2015. Short- and long-term efficacy of forest thinning to mitigate drought impacts in mountain forests in the European Alps. *Ecol. Appl.* 25 (4), 1083–1098.
- Geist, J.M., Cochran, P.H., 1991. Influences of volcanic ash and pumice deposition on productivity of western interior forest soils. In: Harvey, A.E., Neuenschwander, L.F. (Eds.), *Management and Productivity of Western-montane Forest Soils* (Gen. Tech. Rep. INT-280). U.S. Department of Agriculture, Forest Service, Intermountain Research Station, Boise, ID.
- Gilman, E.F., 1990. Tree root growth and development. I. Form, spread, depth and periodicity. *J. Environ. Horticult.* 8 (4), 215–220.
- Hatten, J., Zabowski, D., Ogden, A., Theis, W., Choi, B., 2012. Role of season and interval of prescribed burning on ponderosa pine growth in relation to soil inorganic N and P and moisture. *For. Ecol. Manage.* 269, 106–115.
- Heilman, P.E., Anderson, H.W., Baumgartner, D.M., 1979. *Forest soils of the Douglas-Fir Region*. Washington State University Extension Service, Pullman, WA, pp. 298.
- Hillel, D., 2003. *Introduction to Environmental Soil Physics*. Elsevier Science, Burlington.
- Koraćin, D., Dorman, C.E., Lewis, J.M., Hudson, J.G., Wilcox, E.M., Torregrosa, A., 2014. Marine fog: a review. *Atmos. Res.* 143, 142–175.
- Krueger, E.S., Ochsner, T.E., Engle, D.M., Carlson, J.D., Twidwell, D., Fuhrendorf, S.D., 2015. Soil moisture affects growing-season wildfire size in the southern great plains. *Soil Sci. Soc. Am. J.* 79.
- Liang, X., Lettenmaier, D.P., Wood, E.F., Burges, S.J., 1994. A simple hydrologically based model of land surface water and energy fluxes for general circulation models. *J. Geophys. Res.: Atmos.* 99 (D7), 14415–14428.
- Maeght, J.-L., Rewald, B., Pierret, A., 2013. How to study deep roots—and why it matters. *Front. Plant Sci.* 4, 299.
- Mu, Q., Zhao, M., Running, S.W., 2011. Improvements to a MODIS global terrestrial evapotranspiration algorithm. *Remote Sens. Environ.* 115 (8), 1781–1800.
- Nagarajan, R., 2010. Drought Indices. In: Nagarajan, R. (Ed.), *Drought Assessment*. Springer, Netherlands, pp. 177.
- Noller, J., Ringo, C., Bennett, K., 2018. USDA Forest Service Pacific Northwest Region Soil Resource Inventory. [Internet] Available from: <<https://ecoshare.info/soils/soil-resource-inventory/>> .
- Noy-Meir, I., 1973. Desert ecosystems: environment and producers. *Annu. Rev. Ecol. Syst.* 4 (1), 25–51.
- NRCS, 2008. Soil Quality Indicators Fact Sheet – Available Water Capacity. Available from: <http://www.nrcs.usda.gov/Internet/FSE_DOCUMENTS/nrcs142p2_053288.pdf> .
- Ohmann, J.L., Gregory, M.J., 2002. Predictive mapping of forest composition and structure with direct gradient analysis and nearest-neighbor imputation in coastal Oregon, USA. *Can. J. For. Res.-Revue Canadienne De Recherche Forestiere* 32 (4), 725–741.
- Omernik, J.M., 1987. Ecoregions of the Conterminous United States. Map (scale 1:7,500,000). *Ann. Assoc. Am. Geogr.* 77 (1), 118–125.
- Regalado, C.M., Muñoz Carpena, R., Socorro, A.R., Hernández Moreno, J.M., 2003. Time domain reflectometry models as a tool to understand the dielectric response of volcanic soils. *Geoderma* 117 (3), 313–330.
- Rempe, D.M., Dietrich, W.E., 2018. Direct observations of rock moisture, a hidden component of the hydrologic cycle. *Proc. Natl. Acad. Sci.*
- Sohn, J.A., Gebhardt, T., Ammer, C., Bauhus, J., Häberle, K.-H., Matyssek, R., Grams, T.E.E., 2013. Mitigation of drought by thinning: short-term and long-term effects on growth and physiological performance of Norway spruce (*Picea abies*). *For. Ecol. Manage.* 308, 188–197.
- Soil Survey Staff, 2007. MO-1 Technical Note Number 40 (Revision 1) – NASIS DMU Data Population Guide. Available from: <https://www.nrcs.usda.gov/wps/PA_NRCSConsumption/download?cid=nrcseprd1388227&ext=docx> .
- Soil Survey Staff, 2014. Kellogg soil survey laboratory methods manual. Soil survey investigations report no. 42, Version 5.0. R. Burt and Soil Survey Staff (Eds.), U.S. Department of Agriculture, Natural Resources Conservation Service.
- Soil Survey Staff, 2016a. Gridded Soil Survey Geographic (gSSURGO) Database for the Conterminous United States. [Internet]. Available from: <<https://gdg.sc.egov.usda.gov>> (FY2016 official release).
- Soil Survey Staff, 2016b. Soil Survey Geographic (SSURGO) Database [Internet]. Available from: <<http://sdmdataaccess.nrcs.usda.gov>> (FY2016 official release).
- Soil Survey Staff, 2016c. State Soil Geographic (STATSGO2) Database [Internet]. Available from: <<http://sdmdataaccess.nrcs.usda.gov>> (FY2016 official release).
- Stenger, R., Barkle, G., Burgess, C., 2005. Laboratory calibrations of water content reflectometers and their in-situ verification. *Soil Res.* 43 (5), 607–615.
- Stone, E.L., Kalisz, P.J., 1991. On the maximum extent of tree roots. *For. Ecol. Manage.* 46 (1), 59–102.
- Weitz, A.M., Grauel, W.T., Keller, M., Veldkamp, E., 1997. Calibration of time domain reflectometry technique using undisturbed soil samples from humid tropical soils of volcanic origin. *Water Resour. Res.* 33 (6), 1241–1249.
- Western Regional Climate Center, 2017. Average Statewide Precipitation for Western U.S. States [Internet]. Available from: <https://wrcc.dri.edu/Climate/comp_table_show.php?stype=ppt_avg> .
- Young, K.K., Dixon, J.D., 1966. Overestimation of water content at field capacity from sieved sample data. *Soil Sci.* 101 (2), 104–107.